

Distributed parametric amplifier for RZ-DPSK signal transmission system

Xing Xu, Chi Zhang, T. I. Yuk, and Kenneth K. Y. Wong*

*Photonic Systems Research Laboratory, Department of Electrical and Electronic Engineering,
The University of Hong Kong, Hong Kong*

[*kywong@eee.hku.hk](mailto:kywong@eee.hku.hk)

Abstract: We have experimentally demonstrated a single pump distributed parametric amplification (DPA) system for differential phase shift keying (DPSK) signal in a spool of dispersion-shifted fiber (DSF). The gain spectrum of single pump DPA is thoroughly investigated by both simulation and experiment, and a possible reference for optimal input pump power and fiber length relationship is provided to DPA based applications. Furthermore, DPSK format is compared with on-off keying (OOK) within DPA scheme. Eight WDM signal channels at 10-Gb/s are utilized, and approximately 0.5-dB power penalties at the bit-error rate (BER) of 10^{-9} are achieved for return-to-zero DPSK (RZ-DPSK), comparing to larger than 1.5-dB with OOK format. In order to improve the system power efficiency, at the receiver, the pump is recycled by a photovoltaic cell and the converted energy can be used by potential low-power-consuming devices, i.e sensors or small-scale electronic circuits. Additionally, with suitable components, the whole DPA concept could be directly applied to the 1.3- μm telecommunication window along the most commonly used single-mode fiber (SMF).

© 2012 Optical Society of America

OCIS codes: (190.4970)Parametric oscillators and amplifiers; (060.2330)Fiber optics communications; (060.5060)Phase modulation; (040.5350)Photovoltaic.

References and links

1. G. Kalogerakis, M. E. Marhic, K. K. Y. Wong, and L. G. Kazovsky, "Transmission of optical communication signals by distributed parametric amplification," *J. Lightwave Technol.* **23**(10), 2945–2953 (2005).
2. X. Xu, S. Yang, C. Zhang, T. I. Yuk, and K. K. Y. Wong, "Optically powered communication system with distributed amplifiers," *J. Lightwave Technol.* **28**(21), 3062–3069 (2010).
3. X. Xu, C. Zhang, T. I. Yuk, and K. K. Y. Wong, "Two-Pump Distributed Parametric Amplification for Optically Powered Communication System," in *Optical Fiber Communication Conf.*, Paper OWC7 (2011).
4. M. E. Marhic, N. Kagi, T. K. Chiang, and L. G. Kazovsky, "Broadband fiber optical parametric amplifiers," *Opt. Lett.* **21**(8), 573–575 (1996).
5. J. Boggio, S. Moro, E. Myslivets, J. R. Windmiller, N. Alic, and S. Radic, "155-nm continuous-wave two-pump parametric amplification," *IEEE Photon. Technol. Lett.* **21**(10), 612–614 (2009).
6. Z. Tong, C. Lundstrom, P. A. Andrekson, C. J. McKinstrie, M. Karlsson, D. J. Blessing, E. Tipsuwannakul, B. J. Putnam, H. Toda, and L. Gruner-Nielsen, "Towards ultrasensitive optical links enabled by low-noise phase-sensitive amplifiers," *Nat. Photonics* **5**(7), 430–436 (2011).
7. C. J. McKinstrie, S. Radic, R. M. Jopson, and A. R. Chraplyvy, "Quantum noise limits on optical monitoring with parametric devices," *Opt. Communication* **259**(1), 309–320 (2006).
8. A. Bogris and D. Syvridis, "Distributed Optical Parametric Amplification at 1.3 μm : Performance and Applications in Optical Access Networks," *IEEE Photon. Technol. Lett.* **24**(8), 694–696 (2012).
9. X. Xu, T. I. Yuk, and K. K. Y. Wong, "Distributed Parametric Amplification at 1.3 μm in 25-km Single-Mode Fiber," in *Photon. in Switching*, Paper 0049 (2012).

10. C. Xu, L. Xiang, and W. Xing, "Differential phase-shift keying for high spectral efficiency optical transmissions," *IEEE J. of Selected Topics in Quantum Electron.* **10**(2), 281–293 (2004).
11. A. H. Gnauck and P. J. Winzer, "Optical phase-shift-keyed transmission," *J. Lightwave Technol.* **23**(1), 115–130 (2005).
12. S. Kumar, "Analysis of degenerate four-wave-mixing noise in return-to-zero optical transmission systems including walk-off," *J. Lightwave Technol.* **23**(1), 310–320 (2005).
13. G. W. Lu, K. S. Abedin, T. Miyazaki, and M. E. Marhic, "RZ-DPSK OTDM demultiplexing using fibre optical parametric amplifier with clock-modulated pump," *Electron. Lett.* **45**(4), 221–222 (2009).
14. R. Slavik, F. Parmigiani, J. Kakande, C. Lundstrom, M. Sjodin, P. A. Andrekson, R. Weerasuriya, S. Sygletos, A. D. Ellis, L. Gruner-Nielsen, D. Jakobsen, S. Herstrom, R. Phelan, J. O’Gorman, A. Bogris, D. Syvridis, S. Dasgupta, P. Petropoulos, D. J. Richardson, "All-optical phase and amplitude regenerator for next-generation telecommunications systems," *Nat. Photonics* **4**(10), 690–695 (2010).
15. B. Camille, O. J. W. Andreas, P. P. K. Bill, M. Evgeny, and S. Radic, "320 Gb/s RZ-DPSK Data Multicasting in Self Seeded Parametric Mixer," in *Optical Fiber Communication Conf. 2011, Paper OThC7*.
16. T. Torounidis, H. Sunnerud, P. O. Hedekvist, and P. A. Andrekson, "Amplification of WDM signals in fiber-based optical parametric amplifiers," *IEEE Photon. Technol. Lett.* **15**(8), 1061–1063 (2003).
17. M. E. Marhic, *Fiber Optical Parametric Amplifiers, Oscillators and Related Devices* (Cambridge University Press, 2007).
18. W. Freude, M. Röger, G. Böttger, M. Dreschmann, M. Hubner, C. Klamouris, A.W. Bett, J. Becker, and J. Leuthold, "Optically powered fiber networks," *Opt. Express* **16**(26), 21821–21834 (2008).
19. D. Wake, A. Nkansah, N. J. Gomes, C. Lethien, C. Sion, and J. Vilcot, "Optically Powered Remote Units for Radio-Over-Fiber Systems," *J. Lightwave Technol.* **26**(15), 2484–2491 (2008).
20. M. Roeger, F. Boes, A. Kleff, B. Hiba, M. Baier, M. Hoh, S. Koenig, C. Koos, J. Leuthold, and W. Freude, "Energy-efficient MAC protocol enabling an optically powered sensor network," in *Optical Fiber Communication Conf., Paper JWA088* (2011).

1. Introduction

As one of the promising candidates for distributed amplification system, distributed parametric amplifier (DPA) has been investigated recently [1–3]. Different from traditional fiber based optical parametric amplifier (OPA) which employs highly-nonlinear dispersion-shifted fibers (HNL-DSF) as the amplification medium [4,5], DPA adopts the transmission fibers, thus simultaneous transmission and amplification of signals can be achieved. Meanwhile, as one branch of parametric amplifier, DPA inherits OPA’s intrinsic potential of 0-dB noise figure within the phase-sensitive configuration [6]. During our past work, both single pump [2] and two-pump [3] DPA system were experimentally studied with on-off keying (OOK) signal format. One of the most favorable merits of DPA, comparing to traditional lumped amplifiers, lies in its capability of minimizing the signal power variation along the transmission line, which in return leads to the best tradeoff between the fiber nonlinearities and the noise figure [7]. Additionally, comparing to the widely adopted distributed Raman amplifier (DRA), DPA has several advantages in real applications, i.e. higher power efficiency, free from double Rayleigh scattering (DRS), smaller pump power attenuation and idler generation [1, 2]. As for the power efficiency issue, under the equal gain level assumption, DPA needs much lower pump power than DRA. This is crucial for optical communication systems, since higher pump power means greater safety concern and environmental hazard, not to mention the arising energy saving awareness worldwide. Another potential advantage of DPA is its flexibility, with appropriate optical components, the whole concept could be applied to the 1.3- μm telecommunication window along the most commonly used single-mode fiber (SMF) [8, 9].

When we take signal modulation formats into consideration, utilizing the phase domain of the optical carrier becomes more and more popular, due to the increasing demand of data capabilities for future telecommunication networks [10–15]. With less sensitivity to the fiber nonlinearity effects, phase-shift keying (PSK) is thus more favorable in the WDM transmission system than traditional binary amplitude modulation (OOK). The phase modulation to intensity modulation (PM-IM) conversion from pump to signal, which is always a concern with OOK, will not impair the PSK system, and the phase noise itself could also be minimized in a

phase-sensitive configuration [6]. Moreover, take differential phase-shift keying (DPSK) as an example, it could tolerate large signal power fluctuation with balanced detection, which at the mean time lower the signal-to-noise ratio (SNR) requirement by 3 dB [11].

While in this paper, both numerical and experimental study of single pump DPA gain spectra are investigated in section 2. In the following section we provide a possible reference (input pump power and fiber length relationship) to DPA based applications according to our simulation results. At the receiver, the residual pump recycling further enhance the system performance in terms of the energy efficiency, and the conversion efficiency curve is also shown in section 3. The experimental performance of DPSK and OOK within the same DPA scheme are compared in section 4, around 0.5-dB power penalties at the BER of 10^{-9} are achieved for RZ-DPSK signals with more than 10-dB DPA gain, comparing to larger than 1.5-dB penalties for NRZ-OOK. Finally, we conclude in section 5.

2. DPA gain spectra: simulation and experimental investigation

As described in the introduction, DPA employs transmission fiber as the amplification medium. Thus the fiber loss should be taken into account as in a distributed way. Before the experimental work, in order to further analyze the gain profile of the single pump DPA and later make theoretical comparison with the experimental data, the simulation results of the gain spectra were obtained by the split-step Fourier method (SSFM) within a lossy transmission environment. Key parameters used: (1) pump: 1548.82 nm, 162 mW (22 dBm); (2) signal: -26 dBm; (3) DSF: 10 km, $\gamma = 2 \text{ W}^{-1} \text{ km}^{-1}$, $\alpha = 0.2 \text{ dB/km}$ @ 1550 nm and $\lambda_0 = 1548 \text{ nm}$. The result is shown in Fig. 1(a) (black diamond). Further investigations with the same fiber length were also conducted (Fig. 1(b)). The pump power was increased gradually from 80 mW up to 250 mW. Obvious gain and bandwidth increment can be observed. The results are in accordance with the dependence of OPA gain bandwidth on pump power [17].

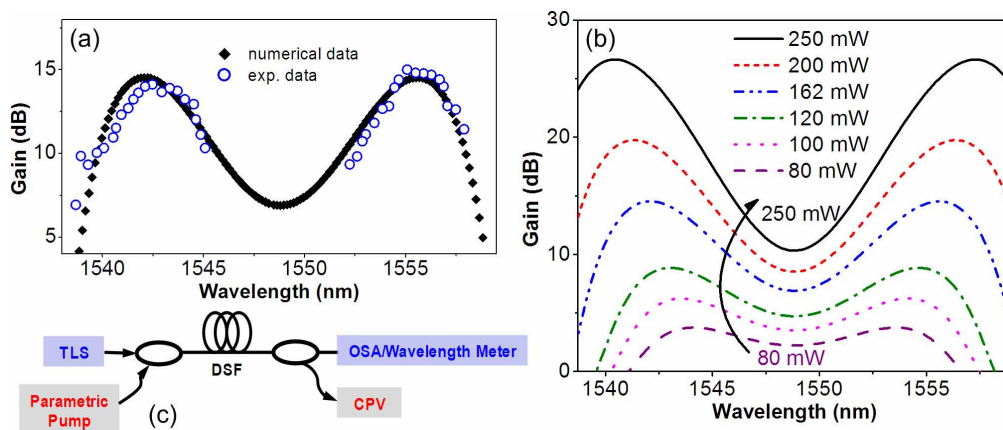


Fig. 1. (a) Experimental (blue circle) and numerical (black diamond) gain spectra with pump @ 1548.82 nm, power of 162 mW and 10-km fiber; (b) Numerical gain spectra with different input pump power (fixed fiber length = 10 km); (c) Experimental scheme for the DPA gain spectrum measurement: TLS: tunable laser source; CPV: concentrated photovoltaic cell.

As for comparison, gain spectrum was experimentally measured and the scheme is shown in Fig. 1(c). The polarizations of both pump and signal branch were aligned by polarization controllers (PC) before the DSF input. The measurement was achieved by scanning one signal source (TLS) from 1538 nm all the way up to 1560 nm (Fig. 1(a), blue circle), while keeping the

pump wavelength (1548.82 nm) and power (162 mW) constant. The gap on between two gain side bands was due to the WDM coupler. Comparatively, for both gain level and bandwidth, the experimental result is in good agreement with the numerical data. However, some discrepancy between theoretical and experimental gain spectra can still be observed in Fig. 1(a), this is mainly due to two factors: (1) the ZDW variations of the 10-km DSF and (2) the polarization drift during the whole measurement process.

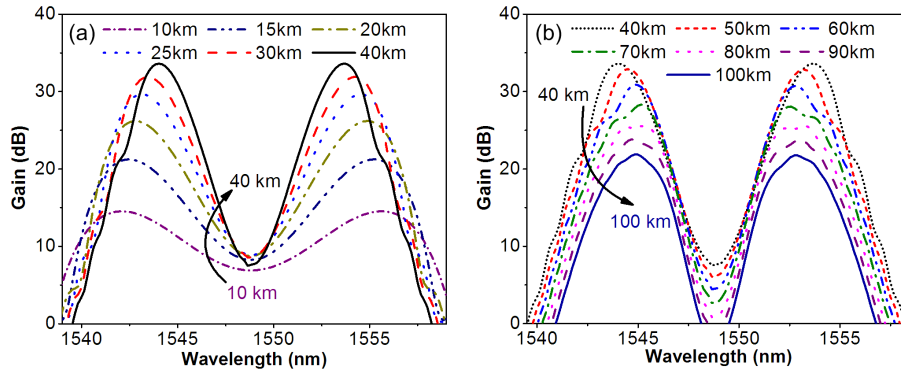


Fig. 2. Numerical gain spectra results with different fiber lengths: (a) 10 to 40 km; (b) 40 to 100 km (pump power = 162 mW).

Since the fiber length was fixed (10 km) and could not be changed for our experiment, simulations with different fiber lengths were conducted and the results are shown in Fig. 2. We gradually increased the fiber length from 10 km to 100 km, while the pump power was maintained at 162 mW. All gain spectra are plotted out in Fig. 2, the peak gain level increased with the fiber length during the first stage (Fig. 2(a), before ~ 41 km), however, at the mean time the gain bandwidth became narrower. Moreover, as we further increased the fiber length, the peak gain level fell off (Fig. 2(b)), this was mainly due to the pump power loss from the fiber attenuation during the transmission process in the DSF. After the highest gain point (~ 41 km), the fiber attenuation for the signal would be larger than the parametric gain within the fiber range beyond 41 km, thus the gain level decreased as the fiber further extended. In our case, with the input pump power at 162 mW, the maximum peak gain appeared when the fiber length reached ~ 41 km, with more than 30-dB gain. The whole gain trend curve with a simulation step of 1 km is shown in Fig. 3(a), together with the residual pump power collected at the fiber output.

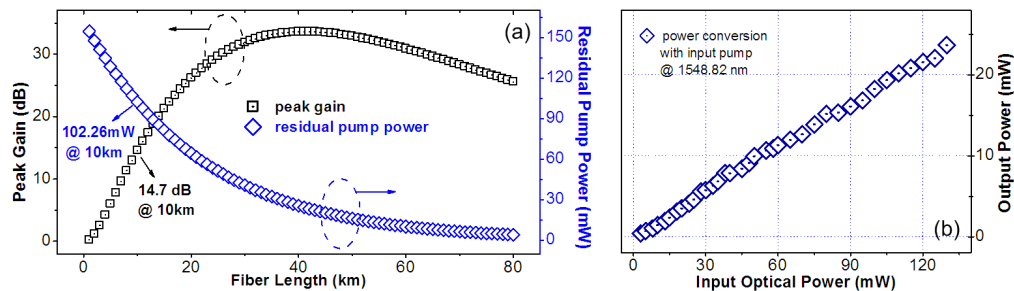


Fig. 3. (a) Peak gains (black square) and residual pump powers (blue diamond) after different fiber lengths with input pump power of 162 mW; (b) Power conversion curve measured @ CPV cell. (pump @ 1548.82 nm)

As shown in the receiver part of Fig. 1(c), one concentrated photovoltaic cell (CPV) was used for residual pump recycling [2, 3]. Figure 3(b) shows the measured conversion curve of CPV cell at the pump wavelength of 1548.82 nm. The average conversion ratio η_{cpv} [2] was 18.3 %, with ≤ 130 -mW input. For the residual pump power of 81.9 mW (19.13 dBm, measured before CPV), the corresponding output was 14.9 mW. Considering the 0.9-dB loss of receiver WDM coupler, the experimental residual pump power: 100.69 mW (19.13 + 0.9 dBm) is well aligned with our numerical data: 102.26 mW (162-mW pump power, 10-km DSF), according to Fig. 3(a). Furthermore, the recycling method can be extended to multi-pump schemes [3] which could provide multiple power sources to different low-power-consuming components including sensors or even cameras [18, 20].

3. Investigation on optimal pump power and fiber length combinations

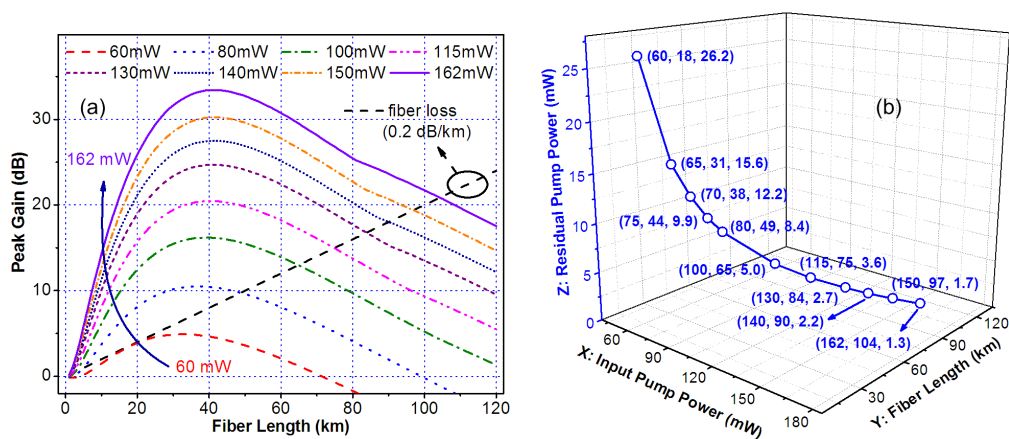


Fig. 4. (a) Peak gains with different fiber lengths and pump powers (60 to 162 mW, @ 1548.82 nm), and the fiber loss slope is 0.2 dB/km (black dash line); (b) Optimal input pump power and fiber length relationship with corresponding residual pump power.

In order to get the whole picture of the gain peak variation trend, we investigated further under the circumstance of both different input pump powers and fiber lengths: pump power: 60 to 162 mW; fiber length: 1 to 120 km (1-km step). The simulation results are shown in Fig. 4(a). As a reference, the loss of the DSF is also depicted out with the slope of 0.2 dB/km as shown in Fig. 4(a). From the perspective of compensating the fiber loss, as a distributed amplifier, the intersections of gain peak curves with the fiber attenuation curve are the optimal pump power points for certain length of transmission fiber, under the assumption of equal input signal power. However, in other occasions, like “last-mile”, optically powered sensor networks or even application into smart power grid [2, 18–20], if we move the focus to both distributed amplification and power recycling aspects, the requirement of fiber extension range is thus shortened to tens of kilometers, hence reasonable residual pump power could be harvested at the fiber output. Under the assumption that peak gain equals to the fiber loss, according to our simulation results, the residual pump powers together with optimal fiber length and input pump power pairs are shown in Fig. 4(b). It can be noticed from the figure that as the pump power increased, the corresponding extension range was also getting longer (from 18 km to 104 km). However, at the mean time, the residual pump power dropped rapidly from 26.2 to 1.3 mW. Furthermore, in practical optical fiber transmission system, if we take other types of power loss [2] into account, i.e. reflected power from SBS, connectors and etc., the recycled

power could be further reduced. According to Fig. 4(b), in order to ensure both transmission loss compensation and residual pump power harvest, it is important to properly choose pump power for different scenarios. The data given in Fig. 4, to some extent, might provide a useful reference to different practical applications based on DPA.

4. Experimental Comparison within DPA system: DPSK vs. OOK

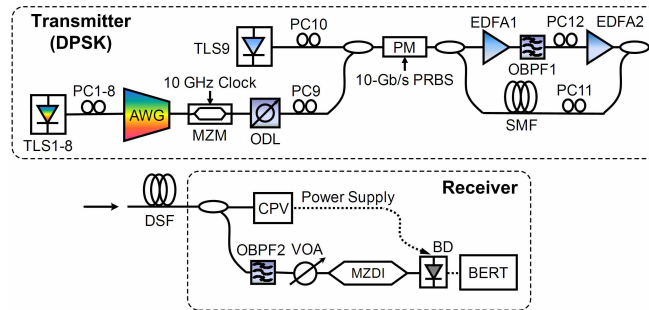


Fig. 5. Experimental setup for DPSK signal format. (abbreviations are defined in the text)

Figure 5 shows the proposed experimental setup of the DPSK signal transmission system. The input WDM signals, wavelength from 1538.94 to 1544.52 nm with the channel spacing of 0.8 nm (100 GHz), were generated by combining the output of eight continuous-wave (CW) tunable laser sources (TLS1-8) with arrayed waveguide grating (AWG) and then intensity-modulating them together by the Mach-Zehnder modulator (MZM), which was driven by a 10-GHz clock pulse train. The polarization controllers (PC1-8) were used to minimize the insertion loss by aligning the corresponding state-of-polarization (SOP) with the transmission axis of the MZM. The modulated signals were further combined with the pump (1548.82 nm) and then phase modulated with a $2^{31}-1$ pseudorandom binary sequence (PRBS) at the phase modulator (PM). The PM was utilized for both the signal data modulation and the pump phase dithering to suppress the stimulated Brillouin scattering (SBS). The tunable optical delay line (ODL) was employed to align the clock signal (@ MZM) with the PRBS (@ PM). A spool of 8-km single-mode fiber (SMF) was deployed to decorrelate WDM channels in the time domain. While for the pump branch, double-stage of erbium-doped fiber amplifiers (EDFA) was applied to boost the pump power up to 24.15 dBm (260 mW). The optical band pass filter (OBPF1) was used to reduce the amplified spontaneous emission (ASE) noise level from EDFA1. One WDM coupler with 3-nm passing band around 1549 nm was used to trim down the ASE noise from EDFA2, and meanwhile combine the pump with the signals. They were then launched together into the DSF (length $L = 10$ km, nonlinear coefficient $\gamma = 2 \text{ W}^{-1}\text{km}^{-1}$ and the zero-dispersion wavelength (ZDW) $\lambda_0 = 1548$ nm). PC 11 and 12 were utilized to align the polarizations of pump and signals before the fiber input. The power level of each WDM channel at fiber input was kept less than -18 dBm. This ensured that the parametric pump was not depleted and the generation of signal-degraded nonlinear effects, i.e., FWM and cross-gain modulation (XGM) [16], would be negligible. At the receiver, signals were demodulated by the Mach-Zehnder delay interferometer (MZDI), and after balanced detector (BD) the performance of each channel was quantified by the bit-error-rate tester (BERT).

The experimental optical spectra for the DPA system with RZ-DPSK WDM signals (8 channels) are shown in Fig. 6. When the parametric pump was switched on (blue solid line in Fig. 6) the corresponding on-off gains for each WDM channel (from channel 1 to 8) were: 12.59 dB (@ 1544.52 nm), 13.64 dB (@ 1543.71 nm), 14.18 dB (@ 1542.90 nm), 12.7 dB (@ 1542.11

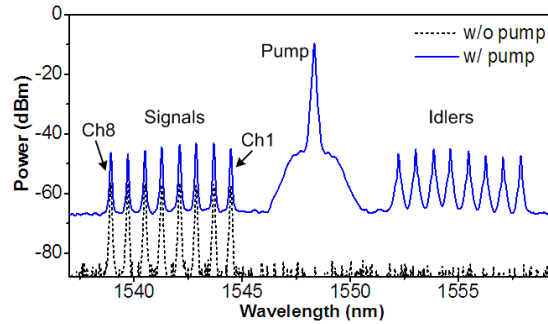


Fig. 6. Optical spectra with (solid line) and without (dotted line) pump. (OSA resolution bandwidth: 0.06 nm)

nm), 12.27 dB (@ 1541.28 nm), 11.04 dB (@ 1540.52 nm), 10.03 dB (@ 1539.72 nm) and 9.91 dB (@ 1538.94 nm), respectively.

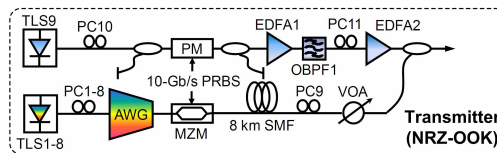


Fig. 7. Experimental setup for NRZ-OOK transmitter. (abbreviations are defined in the text)

The merit of DPSK can not be verified without any experimental comparison to other modulation formats. Thus, as the comparing counterpart, NRZ-OOK signal was also applied into our system with the transmitter setup shown in Fig. 7. The electrical signal feeded into MZM was changed from the clock pulse train into 10-Gb/s $2^{31}-1$ PRBS. The parametric pump branch was kept the same as in the DPSK case (Fig. 5), which ensured equivalent pump power level for both signal formats. By controlling the variable optical attenuator (VOA), the signal power were maintained the same as the DPSK signal at the input of DSF.

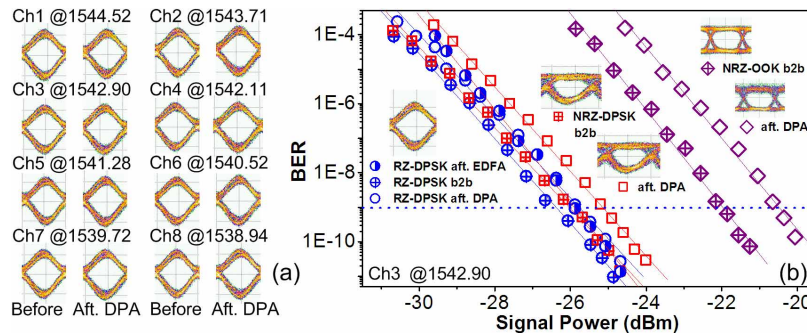


Fig. 8. (a) Eye-diagrams of RZ-DPSK before (left) and after (right) DPA; (b) BER with eye-diagrams of RZ-DPSK after EDFA, NRZ-DPSK and NRZ-OOK (@ 1542.90 nm).

Figure 8(a) list out the eye-diagrams for RZ-DPSK signal before and after amplification. The BER of each WDM channel was measured with all three formats (RZ/NRZ-DPSK and NRZ-OOK), and the results for channel 3 (1542.90 nm) are shown in Fig. 8(b) with the eye-diagrams

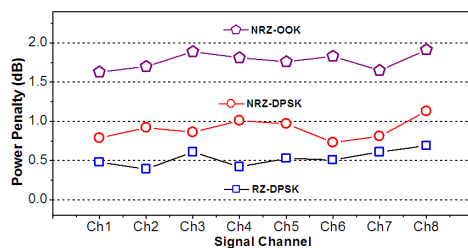


Fig. 9. Power penalties for each WDM channel with 3 different formats.

of NRZ-DPSK and NRZ-OOK. Visible noise and distortions on the mark level of OOK signal could be observed after amplification, which was mainly due to the PM-IM conversion during the parametric amplification process. In contrast, the clear eye openings shown in Fig. 8(a) indicate better tolerance to the effect accompanying the entire parametric process. More quantitatively, around 0.5-dB power penalty at 10^{-9} BER was introduced for the RZ-DPSK signal, and obviously higher value (> 1.5 -dB) were obtained with NRZ-OOK format. As a baseline measurement, EDFA was also applied for RZ-DPSK signal (@ 1542.9 nm) to achieve the same level of on-off gain (14 dB) at the DSF output. According to Fig. 8(b), power penalties measured were 0.48 dB for EDFA and 0.62 dB for DPA, which indicated comparable performance for both amplifiers after 10-km DSF. Error-free operations were achieved for all channels and the power penalties of each channel are plotted out in Fig. 9. These results have experimentally confirmed the advantages of DPSK over OOK within the same DPA circumstances.

5. Conclusions

We have demonstrated an RZ-DPSK WDM signal transmission system with single pump DPA. After both thorough simulations and experimental investigation of the single pump DPA gain spectra, we thus provide a potential reference to DPA based applications with optimal pump power and fiber length relationships. Additionally, the residual parametric pump is recycled by a CPV cell, and the converted energy is further utilized to enhance the power efficiency of the whole system. Detailed comparison of DPSK and OOK format within the same DPA configuration is also presented. The power penalties of approximately 0.5 dB at the BER of 10^{-9} are achieved for RZ-DPSK signal, while more than 1.5-dB penalty occurred with the NRZ-OOK format. Furthermore, with appropriate optical components, the whole concept could be applied to the 1.3- μ m telecommunication window along the most commonly used single-mode fiber (SMF).

Acknowledgments

The work described in this paper was partially supported by grants from the research Grants Council of the Hong Kong Special Administrative Region, China (Project No. HKU 7183/09E).